STRUCTURAL CHEMISTRY

ISSN: 2053-2296
journals.iucr.org/c

Two single-enantiomer amidophosphoesters: a database study on the chirality of $(O)_2P(O)(N)$-based structures

Fahimeh Sabbaghi, Mehrdad Pourayoubi, Marek Nečas and Krishnan Damodaran

Acta Cryst. (2019). C**75**, 77–84

STRUCTURAL CHEMISTRY
ISSN 2053-2296

Two single-enantiomer amidophosphoesters: a database study on the chirality of $(O)_2P(O)(N)$-based structures

Fahimeh Sabbaghi,[a]* Mehrdad Pourayoubi,[b] Marek Nečas[c,d] and Krishnan Damodaran[e]

[a]Department of Chemistry, Zanjan Branch, Islamic Azad University, Zanjan, Iran, [b]Department of Chemistry, Faculty of Science, Ferdowsi University of Mashhad, Mashhad, Iran, [c]Department of Chemistry, Masaryk University, Kotlarska 2, 61137 Brno, Czech Republic, [d]CEITEC – Central European Institute of Technology, Masaryk University, Kamenice 5, 62500 Brno, Czech Republic, and [e]Department of Chemistry, University of Pittsburgh, Pittsburgh, PA 15260, USA. *Correspondence e-mail: fahimeh_sabbaghi@yahoo.com

Received 19 August 2018
Accepted 24 November 2018

Edited by A. R. Kennedy, University of Strathclyde, Scotland

Keywords: single enantiomer; amidophosphoester; phosphate; hydrogen bonding; crystal structure; NMR; diastereotopic.

CCDC references: 1881262; 1881261

Supporting information: this article has supporting information at journals.iucr.org/c

The crystal structures of two single-enantiomer amidophosphoesters with an $(O)_2P(O)(N)$ skeleton, *i.e.* diphenyl [(*R*)-(+)-α-methylbenzylamido]phosphate, (I), and diphenyl [(*S*)-(−)-α-methylbenzylamido]phosphate, (II), both $C_{20}H_{20}NO_3P$, are reported. In both structures, chiral one-dimensional hydrogen-bonded architectures, along [010], are mediated by N—H···OP interactions. The statistically identical assemblies include the noncentrosymmetric graph-set motif $C(4)$ and the compounds crystallize in the chiral space group $P2_1$. As a result of synergistic co-operation from C—H···O interactions, a two-dimensional superstructure is built including a noncentrosymmetric $R_4^4(22)$ hydrogen-bonded motif. A Cambridge Structural Database survey was performed on $(O)_2P(O)(N)$-based structures in order to review the frequency of space groups observed in this family of compounds; the hydrogen-bond motifs in structures with chiral space groups and the types of groups inducing chirality are discussed. The $^{2,3}J_{X-P}$ (X = H or C) coupling constants from the NMR spectra of (I) and (II) have been studied. In each compound, the two diastereotopic C_6H_5O groups are different, which is reflected in the different chemical shifts and some coupling constants.

1. Introduction

Asymmetric induction at phosphorus by a chiral auxiliary group, including an asymmetric C atom, has been demonstrated in single-enantiomer amidophosphoesters, typically including an $(RO)_2P(O)$ segment (R = 2,4-Cl_2-C_6H_3), together with some chiral 2-substituted pyrrolidines (Nakayama & Thompson, 1990). This issue has been established for controlling stereoselectivity in the preparation of optically active phosphate triesters from the corresponding amidophosphoesters, where different reactivities of pro-*S* and pro-*R* *R*O groups are provided.

The amidophosphoester families, especially the chiral ones, are well known for possessing interesting biologicalproperties and for their application in the preparation of different classes of drugs (Warren *et al.*, 2016). Amidophosphoesters have also been used as oxygen-donor ligands in coordination chemistry (Aladzheva *et al.*, 2011) and as flame-retardant compounds in polymer additives (Nguyen & Kim, 2008).

Amidophosphoesters are also interesting for purely scientific studies, for example, the investigation of phosphorus–hydrogen and phosphorus–carbon NMR coupling constants, with examples of short-range $^{2,3}J_{P-H}$ and long-range $^{6,7}J_{P-H}$ coupling constants having been reported (Gholivand *et al.*,

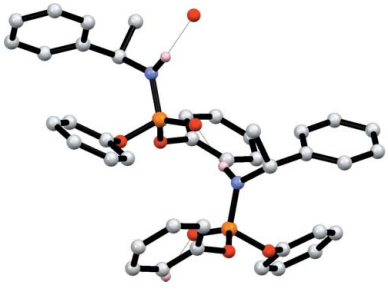

2001, 2005*a*). Differences in the chemical shifts and coupling constants associated with the diastereotopic groups have also been reported (Gholivand *et al.*, 2005*b*; Hamzehee *et al.*, 2016).

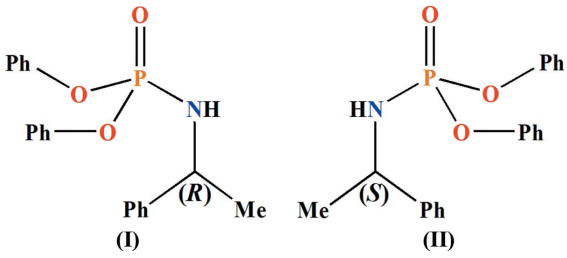

A survey of the Cambridge Structural Database (CSD; Groom *et al.*, 2016) showed the presence of crystal structures of some single-enantiomer compounds with levorotatory or dextrorotatory chiral groups, such as $(C_6H_5O)_2P(O)[NH\text{-}(S)\text{-}(-)\text{-}CH(C_2H_5)(C_6H_5)]$ (Sabbaghi *et al.*, 2011), with no report of two enantiomers, one with an *R* and the other with an *S* chiral group. Such an enantiomeric pair can be of benefit when designing new synthetic methods based on differences in the reactivities of diastereotopic groups.

Following our previous study of two single-enantiomer C(O)NHP(O)-based phosphoric triamide structures (Eghbali Toularoud *et al.*, 2018), we report here the first pair of $(O)_2P(O)(N)$-based enantiomer structures including both chiral *R* and *S* N*RR′* groups. The compounds are $(C_6H_5O)_2P(O)[NH\text{-}(R)\text{-}(+)\text{-}CH(CH_3)(C_6H_5)]$, (I), and $(C_6H_5O)_2P(O)[NH\text{-}(S)\text{-}(-)\text{-}CH(CH_3)(C_6H_5)]$, (II) (see Scheme). The differences between the diastereotopic C_6H_5O groups will be discussed from the point of view of NMR and structural features.

A brief review of analogous structures with the $(O)_2P(O)(N)$ core is also provided from a survey of the CSD. Thus, the frequency of space groups is given, with a discussion of the hydrogen-bond motifs in the structures with chiral space groups and also the types of groups inducing chirality.

The successful preparation of crystals of both (I) and (II) not only provides examples of enantiomerically pure architectures, but may also open up possibilities for designing new chiral ligands for use in coordination chemistry with particular functions or properties. The differences in the reactivities of diastereotopic groups may also be extended to the design of new chiral ligands with diastereotopic chiral donor sites in future.

2. Experimental

2.1. Synthesis and crystallization

The melting point and elemental analysis of $(C_6H_5O)_2P(O)NHCH(CH_3)(C_6H_5)$ were reported previously (Modro *et al.*, 1978). Furthermore, the solvolysis product was studied by ^{1}H NMR spectroscopy in trifluoroacetic acid, where only the coupling constant of the CH_3 proton with phosphorus was reported for the initial compound and for the compound after solvolysis (in both, J = 6 Hz), in addition to the difference between the chemical shifts of the methyl protons for these compounds. Selected MS peaks of $(C_6H_5O)_2P(O)NHCH(CH_3)(C_6H_5)$ were also reported (Davidowitz & Modro, 1984). In these reports, there is no synthesis procedure or any characterization of the $NHCH(CH_3)(C_6H_5)$ fragment as *R*, *S* or racemic.

2.1.1. Preparation of $(C_6H_5O)_2P(O)[NH\text{-}(R)\text{-}(+)\text{-}CH(CH_3)(C_6H_5)]$, (I). For the synthesis of (I), a solution of (*R*)-(+)-α-methylbenzylamine (4 mmol) in dry acetonitrile was added to a solution of diphenylphosphoryl chloride (2 mmol) in the same solvent at 273 K. After stirring for 4 h, the solvent was removed *in vacuo* and the solid obtained was washed with distilled water. Single crystals of (I) suitable for X-ray crystallography were obtained using a mixture of $CHCl_3$ and n-C_7H_{16} (5:1 *v*/*v*) after slow evaporation at room temperature.

Analytical data: m.p. 408 K (literature 377–379 K, from cyclohexane, probably racemic). IR (KBr disc, ν, cm^{-1}): 3182, 3060, 2972, 2887, 1738, 1592, 1488, 1452, 1375, 1311, 1256, 1202, 1161, 1124, 1060, 991, 936, 766, 691. $^{31}P\{^1H\}$ NMR (243 MHz, DMSO-d_6): δ −0.81. ^{1}H NMR (601 MHz, DMSO-d_6): δ 7.38–7.27 (*m*, 6H), 7.29–7.23 (*m*, 2H), 7.22–7.15 (*m*, 4H), 7.14 (*t*, J = 7.4 Hz, 1H), 7.05 (*d*, J = 7.7 Hz, 2H), 6.38 (*dd*, J = 13.6, 9.9 Hz, 1H), 4.45 (*tq*, J = 9.9, 6.8 Hz, 1H), 1.30 (*d*, J = 6.9 Hz, 3H). ^{13}C NMR (151 MHz, DMSO-d_6): δ 150.70 (*d*, J = 6.5 Hz), 150.57 (*d*, J = 6.5 Hz), 145.34 (*d*, J = 4.2 Hz), 129.71, 129.59, 128.10, 126.63, 125.93, 124.72, 124.65, 120.14 (*d*, J = 4.8 Hz), 120.13 (*d*, J = 4.8 Hz), 51.30, 25.07 (*d*, J = 7.4 Hz). MS (70 eV, EI): 353 (15) $[M]^+$, 351 (46) $[M - 2H]^+$, 336 (97) $[M - 2H - CH_3]^+$, 275 (13) $[M - C_6H_6]^+$, 120 (34) $[C_8H_{10}N]^+$, 105 (81) $[C_8H_9]^+$, 77 (100) $[C_6H_5]^+$. UV (CH_3CN, 7.082 × 10^{-6}): λ_{max} = 260 nm, 233 nm. $[\alpha]_D$ = 33° (L = 1 dm, c = 0.0143 g ml^{-1}, $CHCl_3$, T = 291 K).

2.1.2. Preparation of $(C_6H_5O)_2P(O)[NH\text{-}(S)\text{-}(-)\text{-}CH(CH_3)(C_6H_5)]$, (II). Compound (II) was synthesized by a similar method used for the preparation of (I), but using (*S*)-(−)-α-methylbenzylamine instead of (*R*)-(+)-α-methylbenzylamine.

Analytical data: m.p. 410 K. IR (KBr disc, ν, cm^{-1}): 3182, 3064, 2971, 1737, 1590, 1488, 1451, 1372, 1255, 1203, 1125, 1060, 936, 765, 691. $^{31}P\{^1H\}$ NMR (243 MHz, DMSO-d_6): δ −0.81. ^{1}H NMR (601 MHz, DMSO-d_6): δ 7.39–7.33 (*m*, 2H), 7.36–7.28 (*m*, 4H), 7.30–7.23 (*m*, 2H), 7.23–7.11 (*m*, 5H), 7.05 (*d*, J = 7.7 Hz, 2H), 6.39 (*dd*, J = 13.6, 10.0 Hz, 1H), 4.45 (*tq*, J = 10.0, 6.9 Hz, 1H), 1.30 (*d*, J = 6.9 Hz, 3H). ^{13}C NMR (151 MHz, DMSO-d_6): δ 150.64 (*d*, J = 6.5 Hz), 150.51 (*d*, J = 6.6 Hz), 145.29 (*d*, J = 4.1 Hz), 129.63, 129.51, 128.01, 126.54, 125.86, 124.60, 124.53, 120.06 (*d*, J = 4.9 Hz), 120.05 (*d*, J = 4.8 Hz), 51.21, 25.02 (*d*, J = 7.4 Hz). MS (70 eV, EI): 353 (5) $[M]^+$, 351 (84) $[M - 2H]^+$, 335 (97) $[M - 2H - CH_4]^+$, 273 (36) $[M - 2H - C_6H_6]^+$, 120 (100) $[C_8H_{10}N]^+$, 105 (92) $[C_8H_9]^+$, 77 (97) $[C_6H_5]^+$. UV (CH_3CN, 7.082 × 10^{-6}): λ_{max} = 260 nm, 234 nm. $[\alpha]_D$ = −35° (L = 1 dm, c = 0.0082 g ml^{-1}, $CHCl_3$, T = 291 K).

2.2. Refinement

Crystal data, data collection and structure refinement details are summarized in Table 1. For both (I) and (II), all carbon-bound H atoms were placed at calculated positions

Table 1
Experimental details.

	(I)	(II)
Crystal data		
Chemical formula	$C_{20}H_{20}NO_3P$	$C_{20}H_{20}NO_3P$
M_r	353.34	353.34
Crystal system, space group	Monoclinic, $P2_1$	Monoclinic, $P2_1$
Temperature (K)	120	120
a, b, c (Å)	11.3449 (2), 7.3527 (1), 11.8641 (3)	11.3482 (3), 7.3589 (1), 11.8714 (3)
β (°)	113.623 (3)	113.686 (3)
V (Å^3)	906.72 (4)	907.87 (4)
Z	2	2
Radiation type	Mo $K\alpha$	Mo $K\alpha$
μ (mm^{-1})	0.17	0.17
Crystal size (mm)	0.15 × 0.05 × 0.05	0.25 × 0.10 × 0.05
Data collection		
Diffractometer	AFC11 (Right): Eulerian 3 circle CCD	AFC11 (Right): Eulerian 3 circle CCD
Absorption correction	Multi-scan (*CrysAlis PRO*; Rigaku OD, 2015)	Multi-scan (*CrysAlis PRO*; Rigaku OD, 2015)
T_{min}, T_{max}	0.838, 1.000	0.984, 1.000
No. of measured, independent and observed [$I > 2\sigma(I)$] reflections	16344, 3322, 3245	4992, 2908, 2858
R_{int}	0.030	0.015
(sin $\theta/\lambda)_{max}$ (Å^{-1})	0.602	0.602
Refinement		
$R[F^2 > 2\sigma(F^2)]$, $wR(F^2)$, S	0.024, 0.061, 1.07	0.025, 0.069, 1.06
No. of reflections	3322	2908
No. of parameters	230	230
No. of restraints	2	2
H-atom treatment	H atoms treated by a mixture of independent and constrained refinement	H atoms treated by a mixture of independent and constrained refinement
$\Delta\rho_{max}$, $\Delta\rho_{min}$ (e Å^{-3})	0.16, −0.23	0.15, −0.21
Absolute structure	Flack x determined using 1454 quotients $[(I^+) - (I^-)]/[(I^+) + (I^-)]$ (Parsons *et al.*, 2013)	Flack x determined using 1089 quotients $[(I^+) - (I^-)]/[(I^+) + (I^-)]$ (Parsons *et al.*, 2013)
Absolute structure parameter	−0.01 (3)	0.06 (4)

Computer programs: *CrystalClear-SM Expert* (Rigaku, 2014), *CrysAlis PRO* (Rigaku OD, 2015), *SHELXT2014* (Sheldrick, 2015*a*), *SHELXL2018* (Sheldrick, 2015*b*), *Mercury* (Macrae *et al.*, 2008) and *enCIFer* (Allen *et al.*, 2004).

and refined as riding, with their U_{iso} values set at $1.2U_{eq}$ or $1.5U_{eq}$ (for methyl) of the respective carrier atoms; in addition, the methyl H atoms were allowed to rotate about the C—C bond. The nitrogen-bound H atom was located in a difference Fourier map and refined with the U_{iso} value set at $1.2U_{eq}$ of the parent N atom and the N—H bond length restrained to 0.88 (1) Å.

3. Results and discussion

3.1. Description of the crystal structures

Compounds (I) and (II) crystallize to give geometrically and statistically identical crystal structures of opposite handedness. Both structures adopt the monoclinic chiral space group $P2_1$ and the asymmetric units consist of one complete amidophosphoester molecule (Figs. 1 and 2). The molecules in the two structures are very similar to each other apart, of course, from the configuration at the asymmetric C atoms responsible for chirality. The analogous bond lengths and angles are almost equal and the analogous torsion angles have similar values but with opposite signs. The Flack parameters of −0.01 (3) and 0.06 (4) for (I) and (II), respectively, show that the absolute configurations are correct as assigned.

Selected geometric parameters and hydrogen-bond geometries are given in Tables 2–4. The P═O, P—O and P—N bond lengths are within the ranges observed in analogous structures (Hamzehee *et al.*, 2016). The P—N—C and P—O—C angles show a little more '*s*' character with respect to sp^2 hybridization, as has been reported previously by a Cambridge Structural Database (CSD) analysis and by quantum chemical calculations for analogous structures (Sabbaghi *et al.*, 2016; Vahdani Alviri *et al.*, 2018). At the P atom, the narrowest and widest bond angles correspond to O2—P1—O3 and O1—P1—O3, with the values in the structure (I) being typical at 93.09 (7) and 116.47 (8)°, respectively.

Table 2
Comparison of the bond lengths (Å) and angles (°) in (I) and (II).

	(I)	(II)
P1—O1	1.4658 (13)	1.4685 (13)
P1—O3	1.5871 (14)	1.5883 (14)
P1—O2	1.5913 (14)	1.5902 (14)
P1—N1	1.6059 (17)	1.6065 (18)
O1—P1—O3	116.47 (8)	116.45 (8)
O1—P1—O2	116.24 (8)	116.30 (8)
O3—P1—O2	93.09 (7)	93.13 (8)
O1—P1—N1	111.00 (8)	110.92 (9)
O3—P1—N1	110.73 (8)	110.68 (9)
O2—P1—N1	107.94 (8)	108.01 (9)
C9—O2—P1	123.04 (11)	123.17 (12)
C15—O3—P1	122.91 (12)	123.00 (12)
C2—N1—P1	126.51 (13)	126.53 (14)

Table 3
Hydrogen-bond geometry (Å, °) for (I).

D—H···A	D—H	H···A	D···A	D—H···A
N1—H1N···O1^{i}	0.88 (1)	1.94 (1)	2.815 (2)	172 (2)
C7—H7···O2^{ii}	0.95	2.47	3.352 (2)	153

Symmetry codes: (i) $-x, y-\frac{1}{2}, -z$; (ii) $-x+1, y-\frac{1}{2}, -z$.

Table 4
Hydrogen-bond geometry (Å, °) for (II).

D—H···A	D—H	H···A	D···A	D—H···A
N1—H1N···O1^{i}	0.88 (1)	1.96 (1)	2.816 (2)	167 (2)
C7—H7···O2^{ii}	0.95	2.47	3.352 (2)	154

Symmetry codes: (i) $-x+1, y+\frac{1}{2}, -z+1$; (ii) $-x+2, y+\frac{1}{2}, -z+1$.

In the crystal structures of both compounds, molecules are linked by N—H···O hydrogen bonds into zigzag chains that propagate parallel to the *b* axis, and around one of the crystallographic 2_1 axes, as shown in Figs. 3 and 4, building a noncentrosymmetric *C*(4) motif. Considering the weak C—H···O interaction (C7—H7···O2^{ii}; Table 3), a two-dimensional assembly along the *ab* plane is constructed, as shown in Fig. 5 for (I). In this assembly, the noncentrosymmetric hydrogen-bond motif $R_4^4(22)$ is observed [see Fig. 6 for the motif in (I)]. It should be noted that the diastereotopic C_6H_5O groups behave in a different manner in the solid state and while the O2 atom takes part in the weak C—H···O hydrogen-bonding interaction, the O3 atom is far from the possible donor site(s) of the adjacent molecule in the structure.

3.2. CSD analysis

Structures (I) and (II) are examples of chiral structures from chiral molecules. The CSD (Version 5.38, May 2017; Groom *et al.*, 2016) was searched for analogous $(O)_2P(O)(N)$-based structures to determine the variety of space groups, the variation of chiral structures from chiral or achiral molecules, and the most common hydrogen-bonded assemblies in the chiral structures. Metal complexes were not considered and duplicate structures based on the same diffraction data were excluded. After selection, a set of 320 structures was finally considered.

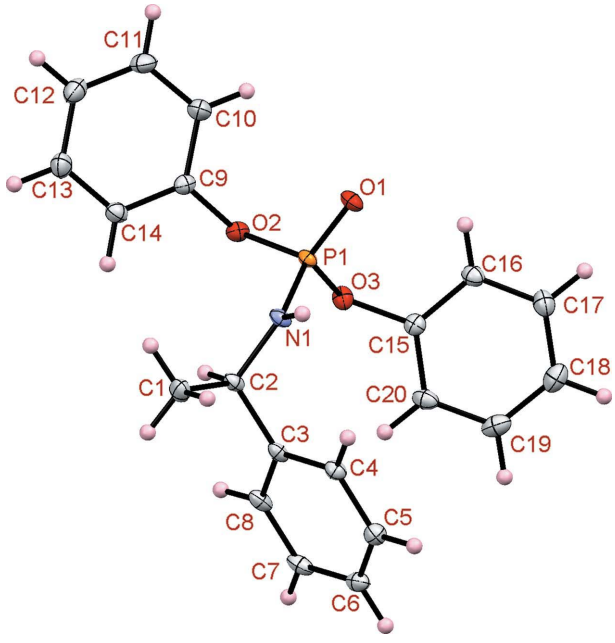

Figure 1
Displacement ellipsoid plot (50% probability level) and the atom-numbering scheme for (I). H atoms are drawn as spheres of arbitrary radii.

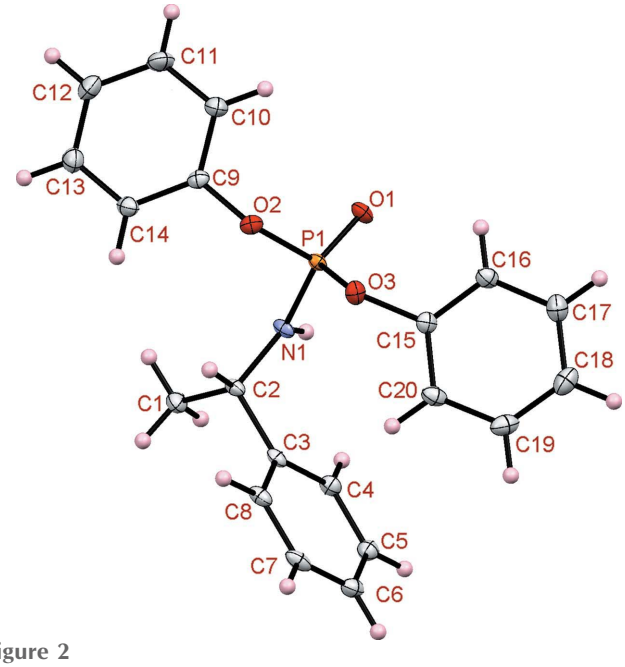

Figure 2
Displacement ellipsoid plot (50% probability level) and the atom-numbering scheme for (II). H atoms are drawn as spheres of arbitrary radii.

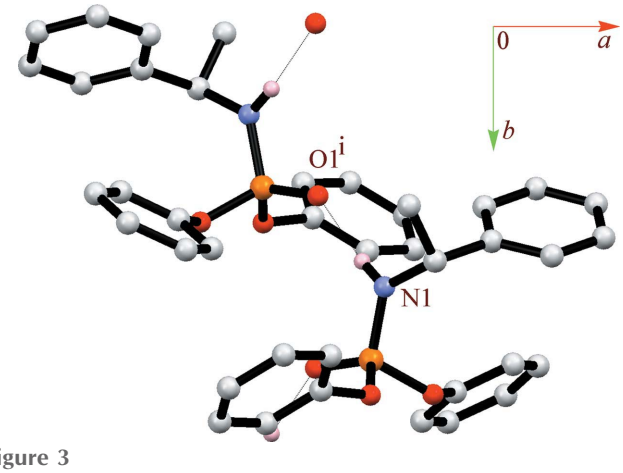

Figure 3
A partial view of the crystal packing of (I), showing the linear hydrogen-bond pattern along the *b* axis. N—H···O hydrogen bonds are shown as dotted lines. C-bound H atoms have been omitted for clarity. [Symmetry code: (i) $-x, y-\frac{1}{2}, -z$.]

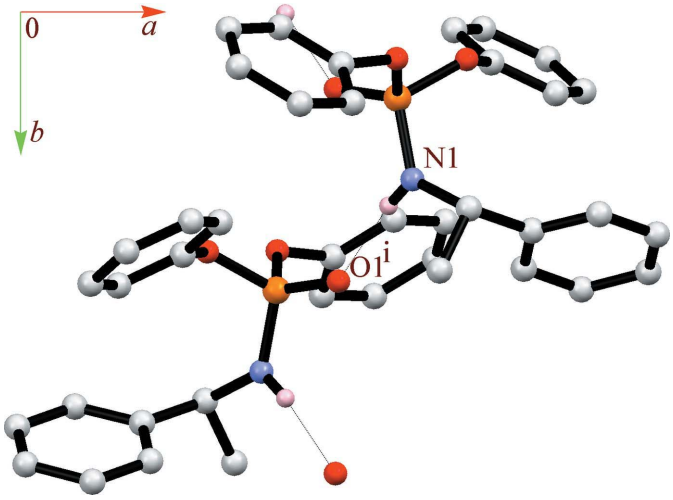

Figure 4
A partial view of the crystal packing of (II), showing the linear hydrogen-bond pattern along the *b* axis. N—H···O hydrogen bonds are shown as dotted lines. C-bound H atoms have been omitted for clarity. [Symmetry code: (i) $-x+1, y+\frac{1}{2}, -z+1$.]

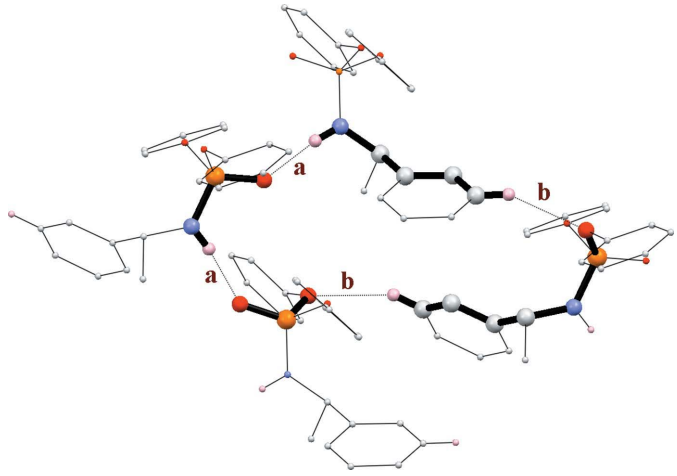

Figure 6
The noncentrosymmetric hydrogen-bond $R_4^4(22)$ motif in the structure of (I). The labels **a** and **b** represent the N1—H1N···O1 and C7—H7···O2 hydrogen bonds (Table 3), respectively; the atoms contributing to the hydrogen-bonded motif are shown in a ball-and-stick representation.

Of the 230 existing space groups (http://www.ccdc.cam.ac.uk/products/csd/statistics), only the following were observed for the $(O)_2P(O)(N)$-based structures: $P2_1/c$, $P\overline{1}$, $P2_12_12_1$, $P2_1$, $C2/c$, $Pbca$, $P1$, Cc, $Pna2_1$, $Pnma$, $Pca2_1$, $Pbcn$, $C2$, $P3_1$, $P4_12_12$, Pn, $P2_12_12$, $P4_1$ and $P4_32_12$. Of these, $P2_1/c$ is found to be the most common and $P\overline{1}$ is the second most common (Fig. S1 in the supporting information). Just these two space groups account for 61% of the surveyed structures, showing the propensity towards crystallization in centrosymmetric crystal structures for $(O)_2P(O)(N)$-based compounds.

In the following paragraphs, the chiral structures are classified according to the segments directing/dictating chirality together with the symmetry preferences of the hydrogen-bond motifs, based on classical hydrogen bonds. Compounds with a unique segment, assembly and structural characteristics are presented and their chemical structures associated with the CSD refcodes are given in Figs. S2–S6 of the supporting information for the subsets defined below.

(*a*) Structures with a single-enantiomer $NHCH(CH_3)(C_6H_5)$ segment, similar to the structures of (I) and (II), typically with *S*-(−) in MAQPID (Hulst *et al.*, 2000) and MIWNUB (Du *et al.*, 2000). There are eight such structures in the CSD, but there is no previous report giving both enantiomers of one compound. For these structures, the following noncentrosymmetric hydrogen-bond motifs are observed based on the N—H···O hydrogen bonds: linear assemblies with a $C_2^2(8)$ graph-set motif, where $Z' = 2$ (FIBROY; Gholivand *et al.*, 2005*b*), and a $C(4)$ motif (MAQPID), and also a noncentrosymmetric $R_2^2(8)$ motif between two symmetry-independent molecules ($Z' = 2$) (MIWNUB). There is also one example of a noncentrosymmetric $C_2^2(6)$ hydrogen-bond motif, based on N—H···O/O—H···O hydrogen bonds, in a structure including a solvent molecule (TUKVOK; Liu *et al.*, 1996); see Fig. S2 of the supporting information. The chiral groups in this subset are well known for asymmetric induction at phosphorus for stereoselectivity usage.

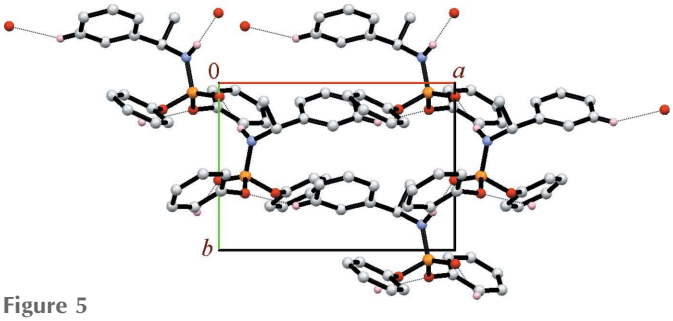

Figure 5
A view of the two-dimensional array of (I) along the *ab* plane formed by N—H···O and C—H···O hydrogen bonds.

(*b*) Structures with chiral segments that are not $NHCH(CH_3)(C_6H_5)$ (see Fig. S3 of the supporting information), including (*S*)-(−)-$NHCH(C_2H_5)(C_6H_5)$ (EXIQIM; Sabbaghi *et al.*, 2011), (*S*)-(−)-2-$CH_3OCH_2(NC_4H_7)$ (KEZTEO; Nakayama & Thompson, 1990), (*S*)-(−)-^{i}PrO–C(O)–$CH(CH_3)$-(NH) [KUSCIM (Chang *et al.*, 2011), UCIXUB (Ross *et al.*, 2011) and PARZIU (Dunn *et al.*, 2017)], (*S*)-$NHCH(CH_3)$-C(O)–O–CH_2CHEt_2 [(ZARNAK; Siegel *et al.*, 2017) and QABZIF (Warren *et al.*, 2016)], (*R*)-$(^i Pr)_2N$–C(═N)[$CH(CH_3)$-(C_6H_5)] (RITZEA; Kim *et al.*, 2007) and L-$NHCH(CH_3)$-C(O)OH (TAFHIR; Xue *et al.*, 1989). The hydrogen-bond motifs found are $C(4)$ and a variety of noncentrosymmetric cyclic motifs. Typical examples of cyclic motifs are $R_4^4(16)$ (KUSCIM), $R_3^3(11)$ (ZARNAK), $R_2^2(8)$ (MIYXAV; Cho *et al.*, 2014) and $R_2^2(10)$ (TAFHIR), with details of the interactions as given in the caption of Fig. S3 of the supporting information. In this subset, the commercially available (*S*)-(−)-$NHCH(C_2H_5)$-(C_6H_5) segment is structurally close to the (*S*)-(−)-NHCH-$(CH_3)(C_6H_5)$ group discussed previously in subset (*a*). For amidophosphoesters including some other chiral segments, the biological properties are well known, typically the commercially available (*S*)-(−)-2-$CH_3OCH_2(NC_4H_7)$ segment exists in some

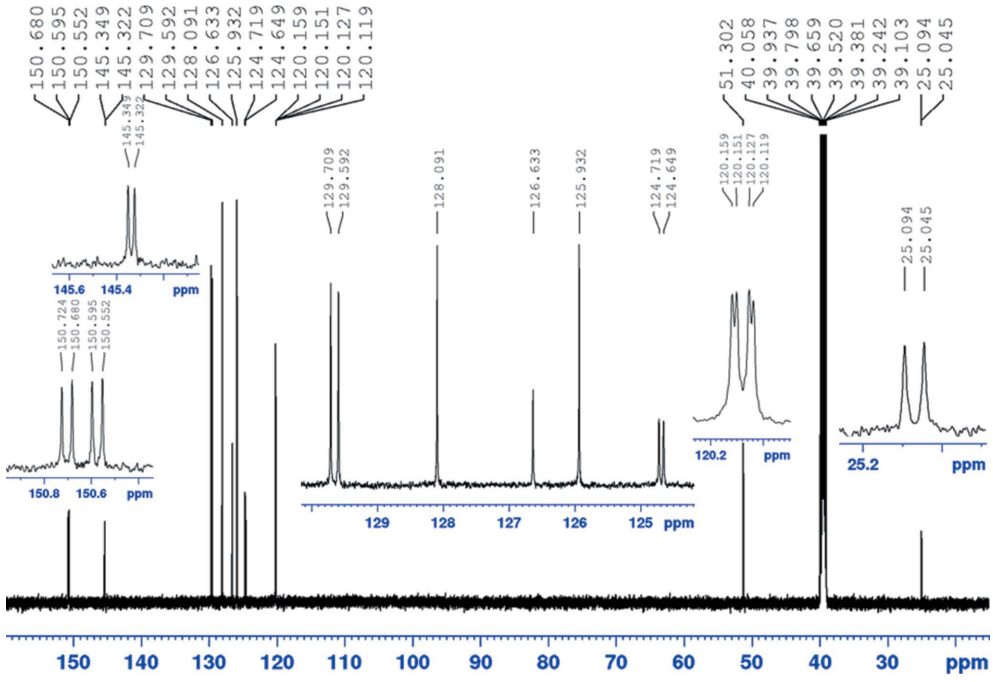

Figure 7
The ^{13}C NMR spectrum of $(C_6H_5O)_2P(O)[NH\text{-}(R)\text{-}(+)\text{-}CH(CH_3)(C_6H_5)]$, (I), in DMSO-$d_6$.

antihepatitis C virus prodrugs (Ross *et al.*, 2011) and a phosphoramide including the synthetic (*S*)-NHCH(CH_3)-C(O)–O–CH_2CHEt_2 segment was reported to have therapeutic efficacy against the Ebola virus (Warren *et al.*, 2016).

(*c*) A group of structures including chiral aromatic diols (Fig. S4 of the supporting information), typically 1,1′-bi-naphthalene-2,2′-diol, for example, CIYVOW (Jiao *et al.*, 2008), MIWNUB (Du *et al.*, 2000) and RITZEA (Kim *et al.*, 2007). In MIWNUB and RITZEA, apart from the chiral diol, there is also a dissymmetric C atom. The hydrogen-bond motifs are not different from those given in the previous subsets and are noncentrosymmetric.

(*d*) A group of compounds with dissymmetry at a P atom (Fig. S5 of the supporting information), for example, in CIHDED (Andrei *et al.*, 2007), PALPHS (Koizumi *et al.*, 1980), two stereoisomers JOFPUP and JOFRAX (Schwalbe *et al.*, 1991), two of OWUYEL and OWUYIP (Morales *et al.*, 2011), and finally in MAQPID (Hulst *et al.*, 2000), with the existence of dissymmetric C atom(s) in some of the examples.

(*e*) A group containing chiral structures obtained from achiral molecules; an inspection of all such structures in the $P(O)(O)_2(N)$ family shows each has one of the following characteristics: (i) the presence of an unsaturated/flexible ring segment in the molecule (most structures in this subset exhibit this characteristic), (ii) the existence of more than one component in the crystal, such as the presence of a solvent molecule, and (iii) the absence of a directing hydrogen bond to form a centrosymmetric hydrogen-bonded motif, or the presence of only weak/nonclassical hydrogen bonds which may lead to a frustration between two or more competing interactions. It has been shown that the frustration between different interactions favours the tendency toward high Z' structures (Anderson *et al.*, 2006), which may also reduce the symmetry of the structure and may not be suitable for the formation of a hydrogen-bond motif including an inversion element, as it is possible to form a dimeric aggregate between two symmetrically independent molecules, and naturally without an inversion element (Torabi Farkhani *et al.*, 2018). The following are examples in this subset: BILCAC (Tarahomi *et al.*, 2013) (flexible ring and no directing hydrogen bond), DAXGIS (Bond *et al.*, 1985) (no directing hydrogen bond) and WIYFAL (Balazs *et al.*, 1999) (including more than one component in the crystal) (Fig. S6 of the supporting information).

Previous publications showed that particular classes of compounds tend to crystallize in noncentrosymmetric crystal structures (Dey & Pidcock, 2008), namely nitroaniline and halopyridine (Desiraju & Krishna, 1988; Etter & Huang, 1992; Saha *et al.*, 2005). In phosphorus-containing compounds, it was reported that substitution of one *ortho* or *meta* H atom on the C_6H_4 phenylene ring would produce asymmetric diaza-phospholes, including a $P(O)(N)_2(1,2\text{-}C_6H_3X)$ segment (*X* is a substituent instead of H), which could pack in acentric space groups (Chemla & Zips, 1987; Barendt *et al.*, 1989). For other examples of chiral space groups from achiral molecules in the $(C)_2P(O)(N)$-based compounds, we note the structures $(C_6H_5)_2P(O)(NH\text{-}cyclo\text{-}C_6H_{11})$ and $(C_6H_5)_2P(O)(NH\text{-}cyclo\text{-}C_7H_{13})$ (Hamzehee *et al.*, 2017), where an unsaturated/flexible ring exists and the hydrogen-bond assembly includes a noncentrosymmetric $C(4)$ motif. For the other family of phosphorus compounds [with an $(O)_2P(S)(N)$ skeleton], $[2,4,6\text{-}(CH_3)_3C_6H_2NH]P(S)[OCH_2CH_3]_2$ is another example of a chiral structure from an achiral molecule, where a frustration between N—H···S and N—H···π interactions leads to a Z' value of 2, with a noncentrosymmetric dimer assembly between two symmetrically-independent molecules (Torabi

Farkhani *et al.*, 2018). In contrast, a previous article showed that the 'carboxylic acid and *cis*-amide dimers prefer centrosymmetric space groups irrespective of the chirality of the molecules' (Dey & Pidcock, 2008).

It should be noted that the expected hydrogen-bond motifs driven by the $(O)_2P(O)NH$ skeleton are a linear chain assembly [$C(4)$ for the structures with $Z' = 1$] or dimeric aggregate [$R_2^2(8)$], built from N—H···O hydrogen bonds. The $R_2^2(8)$ graph-set motif in structures with $Z' = 1$ includes an inversion element and, as a result, a centrosymmetric space group. There are also examples of the existence of other donor/acceptor sites or the presence of solvents which change the hydrogen-bond pattern.

3.3. Spectroscopic study

In the IR spectra of compounds (I) and (II), the band centred at 3182 cm^{-1} is attributed to the NH stretching frequency.

For both (I) and (II), the ^{31}P signal appears at −0.81 ppm, in comparison with the value of 0.05 ppm for the analogous $(C_6H_5O)_2P(O)[NHCH(CH_3)(C_2H_5)]$ compound (Hamzehee *et al.*, 2016).

The NH proton at 6.38/6.39 ppm for (I)/(II) shows a *dd* fine structure, with $^2J_{H-P}$ = 13.6 Hz for both compounds and $^3J_{H-H}$ = 9.9/10.0 Hz in (I)/(II). The two O-phenyl groups are diastereotopic and two sets of peaks are observed for them in the aromatic region. The $^{31}P\{^1H\}$ and ^1H NMR spectra of compound (I) are given in Figs. S7 and S8, respectively (in the supporting information).

In the ^{13}C NMR spectrum, the methyl C atom is observed as a doublet signal, with $^3J_{C-P}$ = 7.4 Hz [25.07/25.02 ppm for (I)/(II)], while the methine C atom does not show any coupling. The other C atom with a three-bond separation from phosphorus at 145.34/145.29 ppm in (I)/(II) shows a doublet with $^3J_{C-P}$ = 4.2/4.1 Hz. For the two diastereotopic C_6H_5O groups, two sets of carbon signals are observed. Typically, the *ipso*-C atoms of phenoxy groups in compound (I) are observed at 150.70 and 150.57 ppm, with a $^2J_{C-P}$ coupling constant of 6.5 Hz for both signals. Similar signals in (II) appear at 150.64 (J = 6.5 Hz) and 150.51 ppm (J = 6.6 Hz). Furthermore, the *ortho*-C atoms at 120.14 and 120.13 ppm in (I) show a $^3J_{C-P}$ coupling constant of 4.8 Hz, and the similar signals for (II) appear at 120.06 (J = 4.9 Hz) and 120.05 ppm (J = 4.8 Hz). The ^{13}C NMR spectrum of compound (I) is shown in Fig. 7.

The mass spectra of both compounds indicate the presence of the molecular ion peak at m/z = 353 in a 70 eV experiment. The ultraviolet (UV) absorption spectra, recorded in acetonitrile, show absorption bands at 260 nm for both compounds and at 233/234 nm for (I)/(II). The bands noted are attributed to the $n\rightarrow\pi^*$ and $\pi\rightarrow\pi^*$ transitions, respectively (Fig. S9 in the supporting information).

3.4. Optical rotation

The specific optical rotations for (I) and (II) are $[\alpha]_D$ = 33 and −35°, respectively, in $CHCl_3$ at T = 291 K. To examine the chiroptical characteristics of these enantiopure compounds in the solution state, the circular dichroism (CD) spectra were investigated for a 2.8 m*M* solution in chloroform (Fig. S10 in supporting information). The CD spectra exhibit opposing signals in (I) and (II), with a near mirror-image relationship with respect to each other. The maximum intensity of the positive peak is observed at 227 nm for (I) and of the negative peak at 226 nm for (II), which are related to the Cotton effect, and conforming to the spectral region characteristic of the π-to-π^* transition bands. The CD sign is negative at wavelengths above 231 nm for (I), while it is positive above 234 nm for (II).

Acknowledgements

Financial support of this work by Zanjan Branch, Islamic Azad University, is gratefully acknowledged.

References

Aladzheva, I. M., Bykhovskaya, O. V., Nelyubina, Y. V., Klemenkova, Z. S., Petrovskii, P. V. & Odinets, I. L. (2011). *Inorg. Chim. Acta*, **373**, 130–136.
Allen, F. H., Johnson, O., Shields, G. P., Smith, B. R. & Towler, M. (2004). *J. Appl. Cryst.* **37**, 335–338.
Anderson, K. M., Afarinkia, K., Yu, H.-W., Goeta, A. E. & Steed, J. W. (2006). *Cryst. Growth Des.* **6**, 2109–2113.
Andrei, M., Bjornstad, V., Langli, G., Romming, C., Klaveness, J., Tasken, K. & Undheim, K. (2007). *Org. Biomol. Chem.* **5**, 2070–2080.
Balazs, G., Drake, J. E., Silvestru, C. & Haiduc, I. (1999). *Inorg. Chim. Acta*, **287**, 61–71.
Barendt, J. M., Bent, E. G., Haltiwanger, R. C., Squier, C. A. & Norman, A. D. (1989). *Inorg. Chem.* **28**, 4425–4427.
Bond, D. R., Modro, T. A., Nassimbeni, L. R. & Wieczorkowski, J. (1985). *Phosphorus Sulfur Relat. Elem.* **22**, 59–69.
Chang, W., *et al.* (2011). *ACS Med. Chem. Lett.* **2**, 130–135.
Chemla, D. S. & Zips, J. (1987). In *Nonlinear Optical Properties of Organic Molecules and Crystals*, Vols. 1 and 2. New York: Academic Press.
Cho, A., *et al.* (2014). *J. Med. Chem.* **57**, 1812–1825.
Davidowitz, B. & Modro, T. A. (1984). *Org. Mass Spectrom.* **19**, 128–134.
Desiraju, G. R. & Krishna, T. S. R. (1988). *Mol. Cryst. Liq. Cryst.* **159**, 277–287.
Dey, A. & Pidcock, E. (2008). *CrystEngComm*, **10**, 1258–1264.
Du, D.-M., Hua, W.-T., Wang, J.-W. & Jin, X.-L. (2000). *Chin. J. Chem.* **18**, 764–769.
Dunn, J. M. M., Reibarkh, M., Sherer, E. C., Orr, R. K., Ruck, R. T., Simmons, B. & Bellomo, A. (2017). *Chem. Sci.* **8**, 2804–2810.
Eghbali Toularoud, M., Pourayoubi, M., Dušek, M., Eigner, V. & Damodaran, K. (2018). *Acta Cryst.* C**74**, 608–617.
Etter, M. C. & Huang, K.-S. (1992). *Chem. Mater.* **4**, 824–827.
Gholivand, K., Ghadimi, S., Naderimanesh, H. & Forouzanfar, A. (2001). *Magn. Reson. Chem.* **39**, 684–688.
Gholivand, K., Shariatinia, Z. & Pourayoubi, M. (2005*a*). *Z. Anorg. Allg. Chem.* **631**, 961–967.
Gholivand, K., Shariatinia, Z. & Pourayoubi, M. (2005*b*). *Z. Naturforsch. Teil B*, **60**, 67–74.
Groom, C. R., Bruno, I. J., Lightfoot, M. P. & Ward, S. C. (2016). *Acta Cryst.* B**72**, 171–179.
Hamzehee, F., Pourayoubi, M. & Choquesillo-Lazarte, D. (2016). *X-ray Struct. Anal. Online*, **32**, 47–48.
Hamzehee, F., Pourayoubi, M., Farhadipour, A. & Choquesillo-Lazarte, D. (2017). *Phosphorus Sulfur Silicon Relat. Elem.* **192**, 359–367.

Hulst, R., Visser, J. M., de Vries, N. K., Zijlstra, R. W. J., Kooijman, H., Smeets, W., Spek, A. L. & Feringa, B. L. (2000). *J. Am. Chem. Soc.* **122**, 3135–3150.
Jiao, P., Nakashima, D. & Yamamoto, H. (2008). *Angew. Chem. Int. Ed.* **47**, 2411–2413.
Kim, S. H., Jung, D. Y. & Chang, S. (2007). *J. Org. Chem.* **72**, 9769–9771.
Koizumi, T., Kobayashi, Y., Yoshii, E., Takamoto, M., Kamiya, K. & Asakawa, H. (1980). *Tetrahedron Lett.* **21**, 3995–3996.
Liu, J., Wang, M., Wang, M.-A., Chen, W.-Y., Shen, Q.-F. & Jin, X.-L. (1996). *Jiegou Huaxue* (*Chin.*) (*Chin. J. Struct. Chem.*), **15**, 486–490.
Macrae, C. F., Bruno, I. J., Chisholm, J. A., Edgington, P. R., McCabe, P., Pidcock, E., Rodriguez-Monge, L., Taylor, R., van de Streek, J. & Wood, P. A. (2008). *J. Appl. Cryst.* **41**, 466–470.
Modro, T. A., Lawry, M. A. & Murphy, E. (1978). *J. Org. Chem.* **43**, 5000–5006.
Morales, E. H. R., Balzarini, J. & Meier, C. (2011). *Chem. Eur. J.* **17**, 1649–1659.
Nakayama, K. & Thompson, W. J. (1990). *J. Am. Chem. Soc.* **112**, 6936–6942.
Nguyen, C. & Kim, J. (2008). *Polym. Degrad. Stabil.* **93**, 1037–1043.
Parsons, S., Flack, H. D. & Wagner, T. (2013). *Acta Cryst.* B**69**, 249–259.
Rigaku (2014). *CrystalClear-SM Expert*. Rigaku Americas Corporation, The Woodlands, Texas, USA.
Rigaku OD (2015). *CrysAlis PRO*. Rigaku Oxford Diffraction Ltd, Yarnton, Oxfordshire, England.
Ross, B. S., Reddy, P. G., Zhang, H.-R., Rachakonda, S. & Sofia, M. J. (2011). *J. Org. Chem.* **76**, 8311–8319.
Sabbaghi, F., Pourayoubi, M., Dušek, M., Eigner, V., Bayat, S., Damodaran, K., Nečas, M. & Kučeráková, M. (2016). *Struct. Chem.* **27**, 1831–1844.
Sabbaghi, F., Pourayoubi, M., Negari, M. & Nečas, M. (2011). *Acta Cryst.* E**67**, o2512.
Saha, B. K., Nangia, A. & Jaskólski, M. (2005). *CrystEngComm*, **7**, 355–358.
Schwalbe, C. H., Chopra, G., Freeman, S., Brown, J. M. & Carey, J. V. (1991). *J. Chem. Soc. Perkin Trans. 2*, pp. 2081–2090.
Sheldrick, G. M. (2015*a*). *Acta Cryst.* A**71**, 3–8.
Sheldrick, G. M. (2015*b*). *Acta Cryst.* C**71**, 3–8.
Siegel, D., *et al.* (2017). *J. Med. Chem.* **60**, 1648–1661.
Tarahhomi, A., Pourayoubi, M., Golen, J. A., Zargaran, P., Elahi, B., Rheingold, A. L., Leyva Ramírez, M. A. & Mancilla Percino, T. (2013). *Acta Cryst.* B**69**, 260–270.
Torabi Farkhani, E., Pourayoubi, M., Izadyar, M., Andreev, P. V. & Shchegravina, E. S. (2018). *Acta Cryst.* C**74**, 847–855.
Vahdani Alviri, B., Pourayoubi, M., Farhadipour, A., Nečas, M. & Bertolasi, V. (2018). *Acta Cryst.* C**74**, 1610–1621.
Warren, T. K., *et al.* (2016). *Nature*, **531**, 381–385.
Xue, C.-B., Yin, Y.-W., Liu, Y.-M., Zhu, N.-J. & Zhao, Y.-F. (1989). *Phosphorus Sulfur Silicon Relat. Elem.* **42**, 149–155.

supporting information

Acta Cryst. (2019). C**75**, 77-84 [https://doi.org/10.1107/S205322961801673X]

Two single-enantiomer amidophosphoesters: a database study on the chirality of $(O)_2P(O)(N)$-based structures

Fahimeh Sabbaghi, Mehrdad Pourayoubi, Marek Nečas and Krishnan Damodaran

Computing details

For both structures, data collection: Rigaku *CrystalClear*-SM Expert 2.1 b32 (Rigaku, 2014) MSCServDetCCD = {5.7.3.4}; cell refinement: *CrysAlis PRO* (Rigaku OD, 2015); data reduction: *CrysAlis PRO* (Rigaku OD, 2015); program(s) used to solve structure: SHELXT2014 (Sheldrick, 2015*a*); program(s) used to refine structure: *SHELXL2018* (Sheldrick, 2015*b*); molecular graphics: *Mercury* (Macrae *et al.*, 2008). Software used to prepare material for publication: *enCIFer* (Allen, *et al.*, 2004 for (I); *enCIFer* (Allen *et al.*, 2004) for (II).

Diphenyl [*R*-(+)-*α*-methylbenzylamido]phosphate (I)

Crystal data

$C_{20}H_{20}NO_3P$
M_r = 353.34
Monoclinic, $P2_1$
a = 11.3449 (2) Å
b = 7.3527 (1) Å
c = 11.8641 (3) Å
β = 113.623 (3)°
V = 906.72 (4) Å^3
Z = 2
$F(000)$ = 372
D_x = 1.294 Mg m^{-3}
Mo $K\alpha$ radiation, λ = 0.71073 Å
Cell parameters from 13845 reflections
θ = 3.4–29.7°
μ = 0.17 mm^{-1}
T = 120 K
Block, colourless
0.15 × 0.05 × 0.05 mm

Data collection

AFC11 (Right): Eulerian 3 circle CCD diffractometer
Radiation source: Rotating Anode MicroMax-007HF DW 1.2 kW
Profile data from ω–scans
Absorption correction: multi-scan (CrysAlis PRO; Rigaku OD, 2015)
T_{min} = 0.838, T_{max} = 1.000
16344 measured reflections
3322 independent reflections
3245 reflections with $I > 2\sigma(I)$
R_{int} = 0.030
θ_{max} = 25.4°, θ_{min} = 3.2°
h = −13→13
k = −8→8
l = −14→14

Refinement

Refinement on F^2
Least-squares matrix: full
$R[F^2 > 2\sigma(F^2)]$ = 0.024
$wR(F^2)$ = 0.061
S = 1.07
3322 reflections
230 parameters
2 restraints
Hydrogen site location: mixed
H atoms treated by a mixture of independent and constrained refinement
$w = 1/[\sigma^2(F_o^2) + (0.0363P)^2 + 0.1116P]$ where $P = (F_o^2 + 2F_c^2)/3$
$(\Delta/\sigma)_{max} < 0.001$
$\Delta\rho_{max}$ = 0.16 e Å^{-3}
$\Delta\rho_{min}$ = −0.23 e Å^{-3}

Absolute structure: Flack *x* determined using 1454 quotients [(I+)-(I-)]/[(I+)+(I-)] (Parsons *et al.*, 2013)
Absolute structure parameter: −0.01 (3)

Special details

Geometry. All esds (except the esd in the dihedral angle between two l.s. planes) are estimated using the full covariance matrix. The cell esds are taken into account individually in the estimation of esds in distances, angles and torsion angles; correlations between esds in cell parameters are only used when they are defined by crystal symmetry. An approximate (isotropic) treatment of cell esds is used for estimating esds involving l.s. planes.

Fractional atomic coordinates and isotropic or equivalent isotropic displacement parameters (Å²)

	x	*y*	*z*	U_{iso}*/U_{eq}
P1	0.11163 (4)	0.55894 (6)	−0.04250 (4)	0.01891 (13)
C1	0.1895 (2)	0.1114 (3)	−0.17193 (19)	0.0317 (5)
H1A	0.117455	0.152536	−0.246310	0.048*
H1B	0.159520	0.017335	−0.131115	0.048*
H1C	0.257187	0.061177	−0.194363	0.048*
O1	−0.00245 (12)	0.5827 (2)	−0.01508 (12)	0.0260 (3)
O2	0.10993 (12)	0.66116 (18)	−0.16137 (12)	0.0241 (3)
C2	0.24293 (18)	0.2716 (3)	−0.08488 (18)	0.0223 (4)
H2	0.271072	0.367118	−0.128810	0.027*
C3	0.35910 (18)	0.2144 (3)	0.02894 (17)	0.0216 (4)
O3	0.23881 (13)	0.6593 (2)	0.04634 (12)	0.0260 (3)
N1	0.13912 (15)	0.3473 (2)	−0.05525 (15)	0.0218 (3)
H1N	0.0931 (19)	0.273 (3)	−0.0303 (19)	0.026*
C20	0.40284 (18)	0.5715 (3)	0.23925 (19)	0.0300 (4)
H20	0.448329	0.514285	0.196962	0.036*
C19	0.4539 (2)	0.5766 (3)	0.3664 (2)	0.0362 (5)
H19	0.534906	0.521430	0.412026	0.043*
C18	0.3878 (2)	0.6614 (3)	0.4276 (2)	0.0380 (5)
H18	0.424179	0.666399	0.514934	0.046*
C17	0.2687 (2)	0.7391 (3)	0.36157 (19)	0.0357 (5)
H17	0.222697	0.794866	0.403915	0.043*
C16	0.21607 (19)	0.7360 (3)	0.23391 (19)	0.0279 (4)
H16	0.135014	0.790819	0.188194	0.033*
C15	0.28415 (18)	0.6514 (3)	0.17465 (18)	0.0234 (4)
C4	0.34404 (18)	0.1152 (3)	0.12231 (17)	0.0242 (4)
H4	0.260152	0.083866	0.115315	0.029*
C5	0.45040 (17)	0.0619 (3)	0.22540 (17)	0.0273 (4)
H5	0.439074	−0.005717	0.288557	0.033*
C6	0.57350 (19)	0.1071 (3)	0.23656 (19)	0.0291 (5)
H6	0.646440	0.071780	0.307487	0.035*
C9	0.00849 (17)	0.6461 (3)	−0.27699 (17)	0.0233 (4)
C8	0.4828 (2)	0.2567 (3)	0.0399 (2)	0.0259 (4)
H8	0.494569	0.322097	−0.023856	0.031*
C7	0.58893 (19)	0.2043 (3)	0.1433 (2)	0.0294 (5)
H7	0.672907	0.235115	0.150359	0.035*

C10	−0.1041 (2)	0.7429 (3)	−0.3018 (2)	0.0320 (5)
H10	−0.115946	0.810978	−0.239135	0.038*
C11	−0.1992 (2)	0.7379 (4)	−0.4207 (2)	0.0387 (5)
H11	−0.277448	0.802145	−0.439333	0.046*
C13	−0.0678 (2)	0.5446 (4)	−0.48532 (18)	0.0348 (5)
H13	−0.055745	0.477124	−0.548126	0.042*
C14	0.02776 (18)	0.5472 (3)	−0.36707 (17)	0.0283 (4)
H14	0.105535	0.481742	−0.348321	0.034*
C12	−0.1809 (2)	0.6405 (4)	−0.5117 (2)	0.0374 (5)
H12	−0.246008	0.639184	−0.592845	0.045*

Atomic displacement parameters (Å²)

	U^{11}	U^{22}	U^{33}	U^{12}	U^{13}	U^{23}
P1	0.0163 (2)	0.0187 (2)	0.0236 (2)	−0.00115 (19)	0.00990 (17)	−0.0023 (2)
C1	0.0416 (11)	0.0266 (12)	0.0279 (10)	0.0053 (9)	0.0148 (9)	−0.0023 (8)
O1	0.0206 (6)	0.0257 (7)	0.0357 (7)	−0.0005 (6)	0.0155 (5)	−0.0062 (6)
O2	0.0207 (6)	0.0224 (7)	0.0285 (7)	−0.0016 (5)	0.0092 (6)	0.0030 (6)
C2	0.0247 (10)	0.0197 (9)	0.0292 (9)	0.0032 (7)	0.0177 (8)	0.0031 (8)
C3	0.0238 (9)	0.0156 (9)	0.0298 (10)	0.0000 (7)	0.0153 (8)	−0.0031 (7)
O3	0.0232 (7)	0.0296 (8)	0.0265 (7)	−0.0086 (6)	0.0114 (6)	−0.0062 (6)
N1	0.0201 (8)	0.0198 (8)	0.0313 (8)	0.0001 (7)	0.0165 (7)	0.0015 (7)
C20	0.0241 (9)	0.0242 (10)	0.0396 (10)	0.0005 (9)	0.0106 (8)	−0.0066 (10)
C19	0.0302 (10)	0.0275 (11)	0.0397 (11)	0.0009 (10)	0.0022 (9)	0.0029 (10)
C18	0.0427 (12)	0.0375 (13)	0.0275 (11)	−0.0070 (11)	0.0076 (10)	0.0014 (10)
C17	0.0382 (12)	0.0409 (13)	0.0314 (11)	−0.0042 (11)	0.0175 (10)	−0.0072 (10)
C16	0.0236 (10)	0.0283 (11)	0.0314 (10)	−0.0005 (9)	0.0104 (9)	−0.0046 (9)
C15	0.0223 (9)	0.0210 (9)	0.0261 (9)	−0.0048 (8)	0.0088 (8)	−0.0026 (8)
C4	0.0215 (9)	0.0233 (10)	0.0299 (10)	−0.0016 (7)	0.0127 (8)	−0.0012 (7)
C5	0.0281 (9)	0.0259 (9)	0.0285 (9)	−0.0005 (10)	0.0121 (8)	0.0000 (10)
C6	0.0231 (9)	0.0267 (11)	0.0333 (10)	0.0037 (8)	0.0070 (8)	−0.0048 (8)
C9	0.0209 (9)	0.0229 (9)	0.0259 (9)	−0.0009 (8)	0.0091 (8)	0.0044 (8)
C8	0.0280 (10)	0.0184 (9)	0.0393 (11)	0.0012 (8)	0.0219 (9)	−0.0007 (9)
C7	0.0205 (9)	0.0240 (10)	0.0474 (12)	−0.0014 (8)	0.0175 (9)	−0.0083 (9)
C10	0.0311 (11)	0.0323 (11)	0.0332 (11)	0.0075 (9)	0.0134 (9)	0.0012 (9)
C11	0.0266 (11)	0.0460 (14)	0.0388 (12)	0.0108 (10)	0.0082 (10)	0.0078 (11)
C13	0.0418 (11)	0.0379 (13)	0.0285 (10)	0.0024 (11)	0.0179 (9)	0.0023 (10)
C14	0.0285 (9)	0.0279 (10)	0.0326 (9)	0.0041 (9)	0.0166 (8)	0.0040 (10)
C12	0.0341 (11)	0.0474 (13)	0.0273 (10)	−0.0003 (10)	0.0085 (9)	0.0063 (10)

Geometric parameters (Å, º)

P1—O1	1.4658 (13)	C17—H17	0.9500
P1—O3	1.5871 (14)	C16—C15	1.383 (3)
P1—O2	1.5913 (14)	C16—H16	0.9500
P1—N1	1.6059 (17)	C4—C5	1.387 (3)
C1—C2	1.523 (3)	C4—H4	0.9500
C1—H1A	0.9800	C5—C6	1.389 (3)

C1—H1B	0.9800	C5—H5	0.9500
C1—H1C	0.9800	C6—C7	1.385 (3)
O2—C9	1.397 (2)	C6—H6	0.9500
C2—N1	1.467 (2)	C9—C14	1.381 (3)
C2—C3	1.520 (3)	C9—C10	1.386 (3)
C2—H2	1.0000	C8—C7	1.385 (3)
C3—C8	1.392 (3)	C8—H8	0.9500
C3—C4	1.393 (3)	C7—H7	0.9500
O3—C15	1.399 (2)	C10—C11	1.391 (3)
N1—H1N	0.883 (13)	C10—H10	0.9500
C20—C19	1.383 (3)	C11—C12	1.380 (3)
C20—C15	1.385 (3)	C11—H11	0.9500
C20—H20	0.9500	C13—C12	1.385 (3)
C19—C18	1.384 (3)	C13—C14	1.388 (3)
C19—H19	0.9500	C13—H13	0.9500
C18—C17	1.385 (3)	C14—H14	0.9500
C18—H18	0.9500	C12—H12	0.9500
C17—C16	1.388 (3)		

O1—P1—O3	116.47 (8)	C15—C16—H16	120.7
O1—P1—O2	116.24 (8)	C17—C16—H16	120.7
O3—P1—O2	93.09 (7)	C16—C15—C20	121.77 (19)
O1—P1—N1	111.00 (8)	C16—C15—O3	119.84 (17)
O3—P1—N1	110.73 (8)	C20—C15—O3	118.15 (17)
O2—P1—N1	107.94 (8)	C5—C4—C3	120.58 (17)
C2—C1—H1A	109.5	C5—C4—H4	119.7
C2—C1—H1B	109.5	C3—C4—H4	119.7
H1A—C1—H1B	109.5	C4—C5—C6	120.17 (19)
C2—C1—H1C	109.5	C4—C5—H5	119.9
H1A—C1—H1C	109.5	C6—C5—H5	119.9
H1B—C1—H1C	109.5	C7—C6—C5	119.41 (19)
C9—O2—P1	123.04 (11)	C7—C6—H6	120.3
N1—C2—C3	112.69 (15)	C5—C6—H6	120.3
N1—C2—C1	108.45 (16)	C14—C9—C10	121.59 (18)
C3—C2—C1	110.84 (16)	C14—C9—O2	118.55 (16)
N1—C2—H2	108.2	C10—C9—O2	119.61 (18)
C3—C2—H2	108.2	C7—C8—C3	120.43 (18)
C1—C2—H2	108.2	C7—C8—H8	119.8
C8—C3—C4	118.89 (18)	C3—C8—H8	119.8
C8—C3—C2	120.26 (16)	C6—C7—C8	120.50 (18)
C4—C3—C2	120.82 (16)	C6—C7—H7	119.8
C15—O3—P1	122.91 (12)	C8—C7—H7	119.8
C2—N1—P1	126.51 (13)	C9—C10—C11	118.5 (2)
C2—N1—H1N	119.1 (16)	C9—C10—H10	120.8
P1—N1—H1N	113.7 (16)	C11—C10—H10	120.8
C19—C20—C15	118.8 (2)	C12—C11—C10	120.5 (2)
C19—C20—H20	120.6	C12—C11—H11	119.7
C15—C20—H20	120.6	C10—C11—H11	119.7

C20—C19—C18	120.4 (2)	C12—C13—C14	120.0 (2)
C20—C19—H19	119.8	C12—C13—H13	120.0
C18—C19—H19	119.8	C14—C13—H13	120.0
C19—C18—C17	120.0 (2)	C9—C14—C13	119.20 (19)
C19—C18—H18	120.0	C9—C14—H14	120.4
C17—C18—H18	120.0	C13—C14—H14	120.4
C18—C17—C16	120.4 (2)	C11—C12—C13	120.2 (2)
C18—C17—H17	119.8	C11—C12—H12	119.9
C16—C17—H17	119.8	C13—C12—H12	119.9
C15—C16—C17	118.59 (19)		

O1—P1—O2—C9	−51.61 (17)	C19—C20—C15—O3	174.51 (19)
O3—P1—O2—C9	−173.24 (15)	P1—O3—C15—C16	−68.4 (2)
N1—P1—O2—C9	73.80 (16)	P1—O3—C15—C20	117.13 (18)
N1—C2—C3—C8	−136.12 (18)	C8—C3—C4—C5	0.9 (3)
C1—C2—C3—C8	102.1 (2)	C2—C3—C4—C5	179.40 (19)
N1—C2—C3—C4	45.4 (2)	C3—C4—C5—C6	0.0 (3)
C1—C2—C3—C4	−76.3 (2)	C4—C5—C6—C7	−0.6 (3)
O1—P1—O3—C15	47.65 (17)	P1—O2—C9—C14	−107.98 (18)
O2—P1—O3—C15	169.09 (15)	P1—O2—C9—C10	77.7 (2)
N1—P1—O3—C15	−80.41 (16)	C4—C3—C8—C7	−1.3 (3)
C3—C2—N1—P1	96.74 (19)	C2—C3—C8—C7	−179.78 (18)
C1—C2—N1—P1	−140.17 (16)	C5—C6—C7—C8	0.3 (3)
O1—P1—N1—C2	178.56 (15)	C3—C8—C7—C6	0.7 (3)
O3—P1—N1—C2	−50.46 (18)	C14—C9—C10—C11	0.4 (3)
O2—P1—N1—C2	50.09 (18)	O2—C9—C10—C11	174.5 (2)
C15—C20—C19—C18	−0.6 (4)	C9—C10—C11—C12	−0.7 (4)
C20—C19—C18—C17	1.2 (4)	C10—C9—C14—C13	0.0 (3)
C19—C18—C17—C16	−1.4 (4)	O2—C9—C14—C13	−174.23 (19)
C18—C17—C16—C15	1.0 (3)	C12—C13—C14—C9	0.0 (3)
C17—C16—C15—C20	−0.4 (3)	C10—C11—C12—C13	0.8 (4)
C17—C16—C15—O3	−174.65 (18)	C14—C13—C12—C11	−0.4 (4)
C19—C20—C15—C16	0.2 (3)		

Hydrogen-bond geometry (Å, º)

D—H···*A*	*D*—H	H···*A*	*D*···*A*	*D*—H···*A*
N1—H1*N*···O1^{i}	0.88 (1)	1.94 (1)	2.815 (2)	172 (2)
C7—H7···O2^{ii}	0.95	2.47	3.352 (2)	153

Symmetry codes: (i) −*x*, *y*−1/2, −*z*; (ii) −*x*+1, *y*−1/2, −*z*.

Diphenyl [(*S*)-(–)-α-methylbenzylamido]phosphate (II)

Crystal data

$C_{20}H_{20}NO_3P$	*b* = 7.3589 (1) Å
M_r = 353.34	*c* = 11.8714 (3) Å
Monoclinic, $P2_1$	β = 113.686 (3)°
a = 11.3482 (3) Å	*V* = 907.87 (4) Å^3

$Z = 2$
$F(000) = 372$
$D_x = 1.293$ Mg m^{-3}
Mo $K\alpha$ radiation, $\lambda = 0.71073$ Å
Cell parameters from 4360 reflections
$\theta = 2.8–29.5°$
$\mu = 0.17$ mm^{-1}
$T = 120$ K
Plate, colourless
0.25 × 0.10 × 0.05 mm

Data collection

AFC11 (Right): Eulerian 3 circle CCD diffractometer
Radiation source: Rotating Anode MicroMax-007HF DW 1.2 kW
Profile data from ω–scans
Absorption correction: multi-scan (CrysAlis PRO; Rigaku OD, 2015)
$T_{min} = 0.984$, $T_{max} = 1.000$
4992 measured reflections
2908 independent reflections
2858 reflections with $I > 2\sigma(I)$
$R_{int} = 0.015$
$\theta_{max} = 25.3°$, $\theta_{min} = 3.2°$
$h = -13 \rightarrow 13$
$k = -8 \rightarrow 7$
$l = -13 \rightarrow 14$

Refinement

Refinement on F^2
Least-squares matrix: full
$R[F^2 > 2\sigma(F^2)] = 0.025$
$wR(F^2) = 0.069$
$S = 1.06$
2908 reflections
230 parameters
2 restraints
Hydrogen site location: mixed
H atoms treated by a mixture of independent and constrained refinement
$w = 1/[\sigma^2(F_o^2) + (0.0462P)^2 + 0.0982P]$ where $P = (F_o^2 + 2F_c^2)/3$
$(\Delta/\sigma)_{max} < 0.001$
$\Delta\rho_{max} = 0.15$ e Å^{-3}
$\Delta\rho_{min} = -0.21$ e Å^{-3}
Absolute structure: Flack x determined using 1089 quotients [(I+)-(I-)]/[(I+)+(I-)] (Parsons *et al.*, 2013)
Absolute structure parameter: 0.06 (4)

Special details

Geometry. All esds (except the esd in the dihedral angle between two l.s. planes) are estimated using the full covariance matrix. The cell esds are taken into account individually in the estimation of esds in distances, angles and torsion angles; correlations between esds in cell parameters are only used when they are defined by crystal symmetry. An approximate (isotropic) treatment of cell esds is used for estimating esds involving l.s. planes.

Fractional atomic coordinates and isotropic or equivalent isotropic displacement parameters (Å^2)

	x	y	z	U_{iso}*/U_{eq}
P1	0.61151 (4)	0.34236 (6)	0.45731 (4)	0.01737 (14)
O1	0.49727 (12)	0.3188 (2)	0.48478 (13)	0.0243 (3)
O2	0.60976 (12)	0.2403 (2)	0.33860 (13)	0.0224 (3)
O3	0.73884 (13)	0.2421 (2)	0.54638 (13)	0.0240 (3)
N1	0.63904 (16)	0.5539 (2)	0.44474 (16)	0.0199 (4)
H1N	0.595 (2)	0.623 (3)	0.4741 (19)	0.024*
C1	0.6890 (2)	0.7906 (3)	0.3279 (2)	0.0298 (5)
H1A	0.756472	0.840944	0.305358	0.045*
H1B	0.659169	0.884371	0.368949	0.045*
H1C	0.616759	0.749541	0.253623	0.045*
C2	0.74292 (18)	0.6298 (3)	0.41504 (18)	0.0201 (4)
H2	0.771108	0.534590	0.371076	0.024*
C3	0.85904 (18)	0.6872 (3)	0.52900 (18)	0.0198 (4)
C4	0.84402 (18)	0.7860 (3)	0.62217 (18)	0.0230 (5)

H4	0.760075	0.816972	0.615132	0.028*
C5	0.95043 (18)	0.8398 (4)	0.72542 (17)	0.0254 (4)
H5	0.939103	0.907449	0.788514	0.030*
C6	1.07343 (19)	0.7947 (3)	0.7364 (2)	0.0273 (5)
H6	1.146384	0.830360	0.807278	0.033*
C7	1.08915 (19)	0.6976 (3)	0.6435 (2)	0.0278 (5)
H7	1.173247	0.667091	0.650786	0.033*
C8	0.9830 (2)	0.6445 (3)	0.5398 (2)	0.0243 (4)
H8	0.994718	0.578894	0.476176	0.029*
C9	0.50822 (18)	0.2553 (3)	0.22246 (18)	0.0217 (4)
C10	0.3956 (2)	0.1584 (3)	0.1978 (2)	0.0293 (5)
H10	0.383639	0.090261	0.260369	0.035*
C11	0.3006 (2)	0.1641 (4)	0.0785 (2)	0.0371 (6)
H11	0.222231	0.100206	0.059562	0.045*
C12	0.3191 (2)	0.2613 (4)	−0.0121 (2)	0.0355 (5)
H12	0.253925	0.262478	−0.093213	0.043*
C13	0.4318 (2)	0.3573 (4)	0.01420 (19)	0.0332 (5)
H13	0.443778	0.424826	−0.048592	0.040*
C14	0.52784 (19)	0.3546 (4)	0.13299 (18)	0.0265 (4)
H14	0.605597	0.420236	0.152039	0.032*
C15	0.78428 (18)	0.2498 (3)	0.67477 (18)	0.0220 (4)
C16	0.71610 (19)	0.1657 (3)	0.73405 (19)	0.0263 (5)
H16	0.634913	0.111176	0.688400	0.032*
C17	0.7690 (2)	0.1628 (4)	0.8619 (2)	0.0340 (5)
H17	0.723324	0.106870	0.904333	0.041*
C18	0.8878 (2)	0.2410 (4)	0.9276 (2)	0.0364 (6)
H18	0.924031	0.236838	1.014889	0.044*
C19	0.9538 (2)	0.3251 (4)	0.8665 (2)	0.0342 (5)
H19	1.034847	0.380043	0.912110	0.041*
C20	0.90283 (18)	0.3298 (3)	0.7393 (2)	0.0283 (5)
H20	0.948318	0.386903	0.697044	0.034*

Atomic displacement parameters (Å²)

	U^{11}	U^{22}	U^{33}	U^{12}	U^{13}	U^{23}
P1	0.0150 (2)	0.0164 (3)	0.0219 (2)	0.00093 (19)	0.00863 (17)	0.0024 (2)
O1	0.0196 (6)	0.0233 (9)	0.0333 (7)	0.0004 (6)	0.0141 (5)	0.0063 (7)
O2	0.0197 (7)	0.0197 (8)	0.0263 (7)	0.0015 (6)	0.0078 (5)	−0.0032 (6)
O3	0.0220 (7)	0.0257 (9)	0.0247 (7)	0.0079 (6)	0.0099 (6)	0.0057 (7)
N1	0.0200 (8)	0.0155 (9)	0.0307 (9)	−0.0001 (7)	0.0168 (7)	−0.0013 (8)
C1	0.0390 (12)	0.0246 (13)	0.0266 (10)	−0.0057 (9)	0.0140 (9)	0.0016 (9)
C2	0.0227 (10)	0.0158 (11)	0.0281 (10)	−0.0028 (7)	0.0167 (8)	−0.0022 (9)
C3	0.0220 (9)	0.0131 (10)	0.0283 (10)	0.0000 (7)	0.0143 (8)	0.0029 (8)
C4	0.0204 (9)	0.0227 (12)	0.0281 (10)	0.0020 (7)	0.0119 (8)	0.0005 (9)
C5	0.0272 (9)	0.0224 (11)	0.0262 (9)	0.0000 (10)	0.0104 (8)	0.0000 (11)
C6	0.0224 (10)	0.0237 (13)	0.0319 (10)	−0.0030 (8)	0.0068 (8)	0.0052 (9)
C7	0.0191 (9)	0.0214 (12)	0.0460 (12)	0.0023 (8)	0.0164 (9)	0.0088 (10)
C8	0.0258 (10)	0.0159 (11)	0.0384 (11)	−0.0011 (8)	0.0205 (9)	0.0010 (10)

C9	0.0202 (9)	0.0196 (10)	0.0248 (9)	0.0003 (8)	0.0087 (8)	−0.0046 (9)
C10	0.0307 (11)	0.0270 (13)	0.0303 (11)	−0.0079 (9)	0.0123 (9)	−0.0024 (10)
C11	0.0255 (11)	0.0442 (16)	0.0365 (12)	−0.0111 (10)	0.0071 (9)	−0.0076 (12)
C12	0.0342 (12)	0.0440 (15)	0.0239 (10)	0.0003 (11)	0.0072 (9)	−0.0069 (11)
C13	0.0392 (12)	0.0359 (15)	0.0274 (10)	−0.0009 (11)	0.0165 (9)	−0.0004 (12)
C14	0.0279 (10)	0.0253 (12)	0.0299 (10)	−0.0052 (9)	0.0155 (8)	−0.0053 (11)
C15	0.0209 (9)	0.0194 (11)	0.0240 (9)	0.0049 (8)	0.0073 (8)	0.0033 (9)
C16	0.0217 (10)	0.0265 (12)	0.0295 (10)	0.0010 (9)	0.0089 (8)	0.0046 (10)
C17	0.0371 (12)	0.0384 (15)	0.0297 (11)	0.0047 (11)	0.0167 (10)	0.0060 (11)
C18	0.0400 (13)	0.0374 (15)	0.0253 (11)	0.0078 (11)	0.0063 (10)	−0.0022 (11)
C19	0.0289 (10)	0.0244 (12)	0.0381 (11)	−0.0009 (10)	0.0018 (8)	−0.0026 (11)
C20	0.0232 (9)	0.0220 (11)	0.0377 (11)	−0.0006 (9)	0.0101 (8)	0.0055 (11)

Geometric parameters (Å, º)

P1—O1	1.4685 (13)	C8—H8	0.9500
P1—O3	1.5883 (14)	C9—C14	1.379 (3)
P1—O2	1.5902 (14)	C9—C10	1.388 (3)
P1—N1	1.6065 (18)	C10—C11	1.394 (3)
O2—C9	1.402 (2)	C10—H10	0.9500
O3—C15	1.400 (2)	C11—C12	1.376 (4)
N1—C2	1.470 (2)	C11—H11	0.9500
N1—H1N	0.875 (12)	C12—C13	1.383 (4)
C1—C2	1.528 (3)	C12—H12	0.9500
C1—H1A	0.9800	C13—C14	1.393 (3)
C1—H1B	0.9800	C13—H13	0.9500
C1—H1C	0.9800	C14—H14	0.9500
C2—C3	1.521 (3)	C15—C16	1.384 (3)
C2—H2	1.0000	C15—C20	1.384 (3)
C3—C4	1.390 (3)	C16—C17	1.390 (3)
C3—C8	1.396 (3)	C16—H16	0.9500
C4—C5	1.389 (3)	C17—C18	1.382 (3)
C4—H4	0.9500	C17—H17	0.9500
C5—C6	1.389 (3)	C18—C19	1.381 (4)
C5—H5	0.9500	C18—H18	0.9500
C6—C7	1.384 (3)	C19—C20	1.383 (3)
C6—H6	0.9500	C19—H19	0.9500
C7—C8	1.389 (3)	C20—H20	0.9500
C7—H7	0.9500		

O1—P1—O3	116.45 (8)	C7—C8—H8	120.0
O1—P1—O2	116.30 (8)	C3—C8—H8	120.0
O3—P1—O2	93.13 (8)	C14—C9—C10	121.99 (19)
O1—P1—N1	110.92 (9)	C14—C9—O2	118.44 (17)
O3—P1—N1	110.68 (9)	C10—C9—O2	119.4 (2)
O2—P1—N1	108.01 (9)	C9—C10—C11	118.0 (2)
C9—O2—P1	123.17 (12)	C9—C10—H10	121.0
C15—O3—P1	123.00 (12)	C11—C10—H10	121.0

C2—N1—P1	126.53 (14)	C12—C11—C10	120.8 (2)
C2—N1—H1N	121.1 (17)	C12—C11—H11	119.6
P1—N1—H1N	111.1 (17)	C10—C11—H11	119.6
C2—C1—H1A	109.5	C11—C12—C13	120.4 (2)
C2—C1—H1B	109.5	C11—C12—H12	119.8
H1A—C1—H1B	109.5	C13—C12—H12	119.8
C2—C1—H1C	109.5	C12—C13—C14	119.8 (2)
H1A—C1—H1C	109.5	C12—C13—H13	120.1
H1B—C1—H1C	109.5	C14—C13—H13	120.1
N1—C2—C3	112.58 (15)	C9—C14—C13	119.0 (2)
N1—C2—C1	108.35 (17)	C9—C14—H14	120.5
C3—C2—C1	110.81 (18)	C13—C14—H14	120.5
N1—C2—H2	108.3	C16—C15—C20	121.78 (19)
C3—C2—H2	108.3	C16—C15—O3	119.93 (18)
C1—C2—H2	108.3	C20—C15—O3	118.08 (18)
C4—C3—C8	119.06 (18)	C15—C16—C17	118.5 (2)
C4—C3—C2	120.91 (17)	C15—C16—H16	120.7
C8—C3—C2	120.02 (18)	C17—C16—H16	120.7
C5—C4—C3	120.69 (18)	C18—C17—C16	120.3 (2)
C5—C4—H4	119.7	C18—C17—H17	119.8
C3—C4—H4	119.7	C16—C17—H17	119.8
C4—C5—C6	120.0 (2)	C19—C18—C17	120.1 (2)
C4—C5—H5	120.0	C19—C18—H18	119.9
C6—C5—H5	120.0	C17—C18—H18	119.9
C7—C6—C5	119.7 (2)	C18—C19—C20	120.5 (2)
C7—C6—H6	120.2	C18—C19—H19	119.8
C5—C6—H6	120.2	C20—C19—H19	119.8
C6—C7—C8	120.52 (19)	C19—C20—C15	118.7 (2)
C6—C7—H7	119.7	C19—C20—H20	120.6
C8—C7—H7	119.7	C15—C20—H20	120.6
C7—C8—C3	120.1 (2)		

O1—P1—O2—C9	51.71 (18)	C2—C3—C8—C7	179.65 (19)
O3—P1—O2—C9	173.36 (16)	P1—O2—C9—C14	107.7 (2)
N1—P1—O2—C9	−73.71 (17)	P1—O2—C9—C10	−77.6 (2)
O1—P1—O3—C15	−47.47 (19)	C14—C9—C10—C11	−0.2 (4)
O2—P1—O3—C15	−169.00 (16)	O2—C9—C10—C11	−174.7 (2)
N1—P1—O3—C15	80.41 (17)	C9—C10—C11—C12	0.8 (4)
O1—P1—N1—C2	−178.52 (16)	C10—C11—C12—C13	−0.9 (4)
O3—P1—N1—C2	50.63 (19)	C11—C12—C13—C14	0.4 (4)
O2—P1—N1—C2	−49.98 (18)	C10—C9—C14—C13	−0.2 (3)
P1—N1—C2—C3	−96.9 (2)	O2—C9—C14—C13	174.3 (2)
P1—N1—C2—C1	140.17 (17)	C12—C13—C14—C9	0.1 (4)
N1—C2—C3—C4	−45.4 (3)	P1—O3—C15—C16	68.2 (3)
C1—C2—C3—C4	76.1 (2)	P1—O3—C15—C20	−117.05 (19)
N1—C2—C3—C8	136.07 (19)	C20—C15—C16—C17	0.1 (3)
C1—C2—C3—C8	−102.4 (2)	O3—C15—C16—C17	174.7 (2)
C8—C3—C4—C5	−0.8 (3)	C15—C16—C17—C18	−0.6 (4)

C2—C3—C4—C5	−179.3 (2)	C16—C17—C18—C19	1.0 (4)
C3—C4—C5—C6	−0.1 (3)	C17—C18—C19—C20	−0.9 (4)
C4—C5—C6—C7	0.6 (4)	C18—C19—C20—C15	0.4 (4)
C5—C6—C7—C8	−0.2 (3)	C16—C15—C20—C19	0.0 (4)
C6—C7—C8—C3	−0.6 (3)	O3—C15—C20—C19	−174.7 (2)
C4—C3—C8—C7	1.1 (3)		

Hydrogen-bond geometry (Å, º)

D—H···*A*	*D*—H	H···*A*	*D*···*A*	*D*—H···*A*
N1—H1*N*···O1^{i}	0.88 (1)	1.96 (1)	2.816 (2)	167 (2)
C7—H7···O2^{ii}	0.95	2.47	3.352 (2)	154

Symmetry codes: (i) −*x*+1, *y*+1/2, −*z*+1; (ii) −*x*+2, *y*+1/2, −*z*+1.